Monthly Notices
of the
ROYAL ASTRONOMICAL SOCIETY

MNRAS **465,** 2143–2150 (2017)
Advance Access publication 2016 November 2

doi:10.1093/mnras/stw2808

Radio light curve of the galaxy possibly associated with FRB 150418

S. Johnston,[1⋆] E. F. Keane,[2,3,4] S. Bhandari,[3,5] J.-P. Macquart,[6] S. J. Tingay,[6,7] E. Barr,[8] C. G. Bassa,[9] R. Beswick,[4] M. Burgay,[10] P. Chandra,[11] M. Honma,[12,13] M. Kramer,[8,4] E. Petroff,[9] A. Possenti,[10] B. W. Stappers[4] and H. Sugai[14]

[1]*CSIRO Astronomy and Space Science, Australia Telescope National Facility, PO Box 76, Epping, NSW 1710, Australia*
[2]*Square Kilometre Array Organisation, Jodrell Bank Observatory, Macclesfield SK11 9DL, UK*
[3]*Centre for Astrophysics and Supercomputing, Swinburne University of Technology, Mail H29, PO Box 218, VIC 3122, Australia*
[4]*Jodrell Bank Centre for Astrophysics, School of Physics and Astronomy, University of Manchester, Manchester M13 9PL, UK*
[5]*Australian Research Council Centre of Excellence for All-sky Astrophysics (CAASTRO), Building A28, School of Physics, The University of Sydney, NSW 2006, Australia*
[6]*International Centre for Radio Astronomy Research (ICRAR), Curtin University, Bentley, WA 6102, Australia*
[7]*Istituto Nazionale di Astrofisica (INAF) – Istituto di Radioastronomia, Via Pietro Gobetti, I-40129 Bologna, Italy*
[8]*Max-Planck-Institut für Radioastronomie (MPIfR), Auf dem Hügel 69, D-53121 Bonn, Germany*
[9]*ASTRON, the Netherlands Institute for Radio Astronomy, Postbus 2, NL-7990 AA Dwingeloo, the Netherlands*
[10]*Istituto Nazionale di Astrofisica (INAF) – Osservatorio Astronomico di Cagliari, Via della Scienza 5, I-09047 Selargius (CA), Italy*
[11]*National Centre for Radio Astrophysics, Tata Institute of Fundamental Research, Pune University Campus, Ganeshkhind, Pune 411 007, India*
[12]*Department of Astronomical Science, SOKENDAI (Graduate University for the Advanced Study), Osawa, Mitaka 181-8588, Japan*
[13]*National Astronomical Observatory of Japan, 2 Chome-21-1 Osawa, Mitaka, Tokyo 181-8588, Japan*
[14]*Kavli Institute for the Physics and Mathematics of the Universe (WPI), Institutes for Advanced Study, University of Tokyo, Kashiwa, Chiba 277-8583, Japan*

Accepted 2016 October 28. Received 2016 October 27; in original form 2016 August 26

ABSTRACT

We present observations made with the Australia Telescope Compact Array (ATCA), the Jansky Very Large Array (JVLA) and the Giant Metre-Wave Telescope of the radio source within the galaxy WISE J071634.59–190039.2, claimed to be host of FRB 150418 by Keane et al. We have established a common flux density scale between the ATCA and JVLA observations, the main result of which is to increase the flux densities obtained by Keane et al. At a frequency of 5.5 GHz, the source has a mean flux density of 140 μJy and is variable on short time-scales with a modulation index of 0.36. Statistical analysis of the flux densities shows that the variations seen are consistent with the refractive interstellar scintillation of the weak active galactic nucleus at the centre of the galaxy. It may therefore be the case that the fast radio burst (FRB) and the galaxy are not associated. However, taking into account the rarity of highly variable sources in the radio sky, and our lack of knowledge of the progenitors of FRBs as a class, the association between WISE J071634.59–190039.2 and FRB 150418 remains a possibility.

Key words: galaxies: active – galaxies: individual: FRB 150418 – galaxies: individual: WISE J071634.59−190039.2.

1 INTRODUCTION

Fast radio bursts (FRBs) are a relatively new class of astrophysical phenomenon, the origin of which remains an open question. Although the Parkes radio telescope has detected the majority of the FRBs (e.g. Lorimer et al. 2007; Keane et al. 2011; Thornton et al. 2013; Burke-Spolaor & Bannister 2014; Petroff et al. 2015b; Ravi, Shannon, & Jameson 2015; Champion et al. 2016; Keane et al. 2016), others have been detected at Arecibo (Spitler et al. 2014) and at the Green Bank Telescope (Masui et al. 2015). Observationally, FRBs are millisecond-duration bursts of radio emission with high dispersion measures (DMs), some of which appear to be polarized. Some FRBs show evidence of scattering, others are temporally unresolved within observational limits while yet others have a double-peaked structure (Champion et al. 2016). FRB 121102 shows multiple bursts with different temporal and spectral features (Scholz et al. 2016; Spitler et al. 2016), whereas extensive observations of other FRBs have failed to see repetition (Lorimer et al. 2007; Petroff et al. 2015b).

The DMs of the FRBs greatly exceed the DM contribution expected from the Milky Way by factors of as much as 30; this has led to the interpretation that the FRBs are extragalactic (Lorimer et al. 2007). In addition, observations of the scattering seen in some

⋆ E-mail: Simon.Johnston@csiro.au

FRBs lends credence to the extragalactic interpretation (Macquart & Johnston 2015; Cordes et al. 2016), whereas the Galactic interpretation (e.g. Loeb, Shvartzvald, & Maoz 2014) seems barely tenable (Dennison 2014). While the extragalactic interpretation of FRBs thus seems reasonably secure, the same cannot be said of their progenitors with many ideas currently in the literature (e.g. Falcke & Rezzolla 2014; Lyubarsky 2014; Cordes & Wasserman 2016; Katz 2016). Indeed, given the observational phenomenology listed above, it remains unclear whether all FRBs have the same origin. If FRBs are indeed extragalactic in origin and can be detected in large numbers at cosmologically interesting distances, they can then be used as tools for high-precision cosmology (McQuinn 2014; Macquart et al. 2015). For example, Keane et al. (2016) used the DM of FRB 150418 in conjunction with the optical redshift of the putative associated galaxy to measure the cosmic density of ionized baryons, and found the result to be in agreement with that of *WMAP* (Hinshaw et al. 2013).

The FRBs in the literature to date have all been discovered with single-dish telescopes and hence have localization of only a few arcmin at best. This means there are many sources at both optical and radio wavelengths within the positional uncertainty of the FRB, making any putative association difficult. Progress in determining the progenitors (or afterglows) of FRBs depends on obtaining an accurate position, and although valiant attempts have been made to detect FRBs with interferometers over a wide range of frequencies (e.g. Wayth et al. 2011; Siemion et al. 2012; Coenen et al. 2014; Karastergiou et al. 2015; Law et al. 2015; Tingay et al. 2015; Burke-Spolaor et al. 2016; Caleb et al. 2016; Rowlinson et al. 2016), arcsecond positions remain elusive.

The SUrvey for Pulsars and Extragalactic Radio Bursts (SUPERB) detected FRB 150418 in real time using the Parkes radio telescope (Keane et al. 2016). Follow-up observations using the Australia Telescope Compact Array (ATCA) and the Subaru optical telescope led to Keane et al. (2016) claiming that a fading radio transient was associated with the galaxy WISE J071634.59−190039.2 at redshift $z = 0.49$. The low probability of finding such a radio source within the field of view of the Parkes telescope (Bell et al. 2015; Mooley et al. 2016) meant that Keane et al. (2016) were able to argue that the transient was associated with the FRB and hence located in the optical galaxy.

Although initially classified as a *transient*, data taken subsequent to the Keane et al. (2016) paper made it clear that the source is more correctly described as a *variable*. This led to the association between the FRB and the radio transient being called into question by Williams & Berger (2016), who claimed that the variability was intrinsic to an active galactic nucleus (AGN), and Akiyama & Johnson (2016), who proposed that the variability was caused by the refractive scintillation of the AGN. Jansky Very large Array (JVLA) observations by Vedantham et al. (2016) covering a wide range of frequencies showed that the radio emission from WISE J071634.59−190039.2 had flux densities comparable to the later epochs of Keane et al. (2016). The source of the emission was shown to be compact on EVN baselines (Giroletti et al. 2016). VLBA and e-MERLIN radio observations and optical imaging with Subaru (Bassa et al. 2016) showed that the compact radio source is located in the centre of WISE J071634.59−190039.2 and suggested that the source is likely a weak AGN.

In this paper, we describe observations of the radio source performed with the ATCA, the JVLA and the Giant Metre Wave Telescope (GMRT) in Section 2. Section 3 presents the results with special attention given to the absolute flux density calibration between the ATCA and JVLA observations. Section 4 is dedicated to an interpretation of the radio light curve before we present our conclusions in Section 5.

2 OBSERVATIONS AND DATA REDUCTION

Observations of the field containing FRB 150418 were made with the ATCA, the GMRT and the JVLA covering a period of close to one year after the FRB. In addition, JVLA observations were made by Williams & Berger (2016) and Vedantham et al. (2016) following the publication of Keane et al. (2016). A series of observations were also made with the VLBA and e-MERLIN, described in detail in Bassa et al. (2016), and with the EVN (Giroletti et al. 2016).

A total of 10 epochs were obtained with the ATCA of which the first five were included in Keane et al. (2016). Their observations plus those of epoch 6 were made by mosaicking together 42 separate pointings. For epochs 7–10 inclusive, a single pointing was used centred on the position of the WISE galaxy. All these observations were carried out in two bands each of 2-GHz bandwidth, the first centred at 5.5 GHz and the second at 7.5 GHz. Flux calibration was carried out with the ATCA calibrator B0823−500, while phase calibration was performed using B0733−174. ATCA data reduction was carried out using the MIRIAD package (Sault, Teuben, & Wright 1995) using standard techniques. For the mosaicked observations, each pointing was reduced separately and the pointings later combined using the task LINMOS. Each 2-GHz band was reduced independently. Flux measurements were made using the task IMFIT from the images and UVFIT directly from the calibrated UV data.

Three epochs were obtained with the GMRT. The first and second epochs used 3C286 as the flux calibrator, whereas the third epoch used 3C147. Phase calibration was carried out using 0837–198 for the first epoch and 0735–175 for the last two epochs. GMRT data reduction was carried out using AIPS, and the images were then ported into MIRIAD for analysis.

A single epoch was obtained with the JVLA. A seven-point mosaic was used to tile the field of view surrounding the FRB. A total of 4 GHz of bandwidth was used centred at 6.0 GHz. Flux calibration was carried out with 3C147 and phase calibration with B0733−174, the same phase calibrator as used for the ATCA. Interference flagging and imaging were carried out using CASA.

Finally, the data taken by Williams & Berger (2016) on the JVLA became publicly available and were reanalysed. These observations were made with a single pointing in two separate bands each with 1 GHz bandwidth centred at 5.5 and 7.5 GHz. Again, 3C147 and B0733−174 were used for flux and phase calibration. Data reduction was carried out using CASA. The images were ported into MIRIAD, and flux density measurements were made using the task IMFIT in an identical fashion to the ATCA data.

In this paper, flux densities were obtained using IMFIT under the assumption that the source is unresolved at the observing frequencies and baseline lengths of the ATCA, GMRT and JVLA, an assumption justified by the long baseline results (Bassa et al. 2016).

2.1 Absolute flux density calibration

The ATCA data described in Keane et al. (2016) and those subsequently obtained on the ATCA were flux density calibrated using B0823−500, as the source was in angular proximity to the FRB field, whereas the primary ATCA flux density calibrator B1934−638 was not. We did, however, also observe B1934−638

on most occasions. B0823−500 is known to have intrinsic variability on yearly time-scales, and, indeed, its flux density has been increasing over the last decade, making the flux density model built into MIRIAD out of date (J. Stevens, private communication). To quantify this effect, we separately measured the flux density of the phase calibrator B0733−174 using B0823−500 or B1934−638 as the flux calibrator. We found that at 5.5 GHz, the use of B0823−500 underestimates flux density measurements by on average 8 per cent, whereas at 7.5 GHz, this difference is 15 per cent. We see only a marginal increase in the flux density of B0823−500 over the entire data span. The flux densities described in Keane et al. (2016) therefore, although self-consistent, are too low by these amounts for the purposes of absolute comparison with other instruments.

In addition to this effect, we have uncovered an issue with the way that MIRIAD deals with the primary beam correction for mosaicked images over wide bandwidths such as used in these observations. The consequence of this effect is that the flux densities as measured with mosaicked images are lower than those made with a single pointing. To quantify this effect, we took advantage of other sources within the field of view of the large mosaic. We compared the flux densities as measured with the mosaic with those measured when dealing solely with the single pointing containing the source. We find that the flux densities of the single pointings are 10 per cent higher than those in the mosaics because of the way MIRIAD handles a large fractional bandwidth in the LINMOS routine. A similar effect also appears to be present in the CASA reduction of JVLA mosaics and affects the flux density that we measured in those observations. We therefore also extracted the single pointing of the JVLA mosaic that contained the WISE galaxy and processed these data independently.

For the ATCA data, the two bands (from 4.5 to 6.5 GHz and from 6.5 to 8.5 GHz) are treated independently. We have verified the calibration between the two bands by examining the spectrum of the phase calibrator, to ensure that it forms a smooth power law over the entire 4 GHz range.

Finally, in order to compare the JVLA and ATCA observations, we need to ensure that there is overlap in the frequency coverage. The JVLA observation taken by us from 4.0 to 8.0 Hz is offset from the ATCA observations from 4.5 to 8.5 GHz. The JVLA observations of Williams & Berger (2016) were centred at the same frequencies as the ATCA but had only 1 GHz of bandwidth per sub-band, rather than the 2 GHz of the ATCA. Given the spectral behaviour of this source, it is important to keep these differences in mind when trying to compare flux density measurements from the different observations.

2.2 Summary of data calibration

In summary, the flux density values presented in Keane et al. (2016) are self-consistent between epochs but are, in absolute terms, low for two reasons. First, MIRIAD has an incorrect model for the (current) flux density of B0823−500, and, secondly, MIRIAD incorrectly accounts for primary beam correction across a wide bandwidth for mosaicked images. The total of these effects means that the Keane et al. (2016) flux densities are too low by about 20 per cent in comparison to those obtained with the JVLA. If we require an accuracy of a greater than 10 per cent level, all these effects need to be accounted for.

Potential pitfalls of measuring flux density have been described in great detail in Rau, Bhatnagar, & Owen (2016). Effects include clean bias, interference flagging, imaging algorithms used (MIRIAD versus CASA), the effects of wide bands and the software used to compute flux densities in either the image or the uv domain. These effects are likely to account for most of the residual differences between measurements noted below.

3 RESULTS

Table 1 lists the observations and the measurements of the flux density of WISE J071634.59−190039.2. Note that the date of the fourth epoch of ATCA observations is 2015 July 4 and not June 4, as reported in Keane et al. (2016). Where the source was not detected at 7.5 GHz, we give a 3σ upper limit. The source was not detected in any of the GMRT observations, and we quote an upper limit likewise.

In Table 2, we compare the flux density obtained with the JVLA data, as reported in Williams & Berger (2016), with those obtained through data reduction carried out by us. These agree within the 1σ error bars apart from the data taken on 2016 March 23. We note that there is a discrepancy between the result in the published paper at this epoch (218 ± 24 μJy) and that given in ATEL #8946 (185 ± 18 μJy), with the latter value consistent with our value. In subsequent analyses, we use the values that we derived.

We note that the brightness obtained with the VLBA on 2016 March 8 of 151 ± 15 μJy beam^{-1} is significantly lower than that obtained only 17 h later with the JVLA (192 ± 17 μJy), and the EVN brightness on 2016 March 16 was 125 ± 22 μJy beam^{-1} as opposed to the JVLA value of 254 ± 15 μJy taken only a few hours later. One possible interpretation is that the EVN and VLBA are resolving the structure, leading to a lower brightness. We do not believe this to be the case, however, as the intermediate-resolution data from e-MERLIN are consistent with both the ATCA/JVLA and the EVN/VLBA measurements.

The left-hand panel of Fig. 1 shows the light curve at 5.5 GHz. Red points are values obtained with the ATCA, blue points from the JVLA, and green points from VLBA, e-MERLIN (Bassa et al. 2016) and the EVN (Giroletti et al. 2016). The right-hand panel of the figure shows the 5.5- and 7.5-GHz light curves from measurements taken on the ATCA. It can clearly be seen that the first two epochs have a strongly falling spectrum (negative spectral index), whereas for epochs 3–7, the spectrum is flat. Fig. 2 shows in more detail the final 100 d of observations.

For the ATCA observations from epochs 7 to 10, where only single pointings of a long duration were obtained, the signal-to-noise ratio of the radio source is significantly higher than in the earlier epochs. This allows the data to be subdivided into frequency and time bins. Fig. 3 shows the spectra for these four epochs. The spectral index is highly variable. Finally, Fig. 4 shows the flux density as a function of time for epochs 7–10 at both 5.5 and 7.5 GHz. For each epoch, we subdivide the data into 2.5 h time averages in steps of 1.25 h. At 5.5 GHz, there is marginal evidence for variability on the time-scale of a few hours but nothing like the factor of 2 change between the measurements on the JVLA and EVN on 2016 March 16. At 7.5 GHz significant time variability is seen from epoch to epoch.

4 DISCUSSION

4.1 Variability

For a formal metric for variability, we use the debiased modulation index, $m_{\rm d}$, and χ^2 statistic from Bell et al. (2015), as well as the

Table 1. Observations and flux density of the radio source associated with WISE J071634.59–190039.2.

Date	Start (UT)	Length (h)	MJD	Telescope	Band (GHz)	Array	Mode	Flux density (μJy)	Error
2015 April 18	06:30	5.5	571 30.271	ATCA	4.5–6.5	6A	Mosaic	320	18
					6.5–8.5	6A	Mosaic	225	27
2015 April 24	02:44	12.0	571 36.114	ATCA	4.5–6.5	6A	Mosaic	154	19
					6.5–8.5	6A	Mosaic	<90	30
2015 April 26	01:45	10.0	571 38.073	ATCA	4.5–6.5	6A	Mosaic	106	17
					6.5–8.5	6A	Mosaic	<90	30
2015 May 18	12:30	2.0	571 59.521	GMRT	0.69–0.72		Single	<350	
2015 May 22	12:42	2.0	571 63.529	GMRT	1.37–1.40		Single	<150	
2015 July 04	21:12	7.4	572 08.884	ATCA	4.5–6.5	6D	Mosaic	98	17
					6.5–8.5	6D	Mosaic	<90	30
2015 October 27	14:09	8.5	573 22.59	ATCA	4.5–6.5	6D	Mosaic	98	17
					6.5–8.5	6D	Mosaic	<75	25
2015 November 11	18:40	8.5	573 36.778	GMRT	1.37–1.40		Single	<70	
2016 February 24	06:09	7.6	574 42.4	ATCA	4.5–6.5	6B	Mosaic	106	13
					6.5–8.5	6B	Mosaic	<75	25
2016 March 01	04:18	1.2	574 48.17	JVLA	4.0–8.0	C	Mosaic	132	10
2016 March 01	05:29	11.0	574 48.5	ATCA	4.5–6.5	6B	Single	121	6
					6.5–8.5	6B	Single	111	8
2016 March 10	10:29	5.0	574 57.5	ATCA	4.5–6.5	6B	Single	143	6
					6.5–8.5	6B	Single	59	8
2016 March 11	10:25	5.0	574 58.5	ATCA	4.5–6.5	6B	Single	140	6
					6.5–8.5	6B	Single	225	11
2016 March 13	10:23	5.0	574 60.5	ATCA	4.5–6.5	6B	Single	137	6
					6.5–8.5	6B	Single	156	11

Table 2. Flux density at 5.5 GHz of the radio source associated with WISE J071634.59–190039.2 from observations taken on the JVLA by Williams & Berger (2016). For 2016 March 23, we use their published value rather than the ATEL value.

Date	Start (UT)	Length (h)	MJD	Flux density (μJy) (Williams & Berger)	Error	Flux density (μJy) (this paper)	Error
2016 February 27	00:25	1.5	574 45.03	156	11	169	17
2016 February 28	00:11	1.5	574 46.02	153	13	165	17
2016 March 5	00:07	0.5	574 52.02	105	21	116	14
2016 March 8	23:54	0.5	574 56.01	225	24	192	17
2016 March 11	23:29	0.5	574 58.99	147	26	151	14
2016 March 16	23:04	0.5	574 63.97	279	25	254	15
2016 March 23	22:58	0.5	574 70.97	218	24	153	16
2016 March 28	22:52	0.5	574 75.97	259	21	221	16
2016 March 31	23:12	0.5	574 78.98	205	15	189	11
2016 April 1	22:00	0.5	574 79.93	260	34	270	28

variability statistic, V_S, from Mooley et al. (2016). These are defined by

$$m_d = \frac{1}{\overline{S}}\sqrt{\frac{\sum_{i=1}^{n}(S_i - \overline{S})^2 - \sum_{i=1}^{n}\sigma_i^2}{n}}, \quad (1)$$

$$\chi^2_{lc} = \sum_{i=1}^{n}\frac{(S_i - \tilde{S})^2}{\sigma_i^2}, \quad (2)$$

$$V_S = \frac{S_{max} - S_{min}}{\sigma}, \quad (3)$$

where n is the number of data points, S_i and σ_i are the flux density and the error bar for each datum, $\overline{S}$ and $\tilde{S}$ are the mean and weighted mean flux densities, and S_{max} and S_{min} are the maximum and minimum flux densities recorded.

Combining the data taken at 5.5 GHz with the ATCA and the JVLA, $\tilde{S} = 140$ μJy, $m_d = 0.36$, $\chi^2 = 250$ and $V_S = 11$. These values change only slightly if the e-MERLIN and VLBA points from Bassa et al. (2016) are included. We note that, in spite of our best efforts at determining the absolute calibration, $\tilde{S}$ for the Williams & Berger (2016) data (181 μJy) is significantly larger than the ATCA data. The data taken at 7.5 GHz at later epochs yield $\tilde{S} = 120$ μJy, $m_d = 0.39$, $\chi^2 = 180$ and $V_S = 12$. Both the modulation indices and the variability time-scales are in line with those predicted by Akiyama & Johnson (2016) at these Galactic latitudes.

Observationally, a source with these variability metrics is rare, and, by these measures, both Bell et al. (2015) and Mooley et al. (2016) would clearly classify this source as a variable. Ofek et al. (2011) have only 12 out of 464 sources (∼0.5 per cent) with χ^2 greater than 100; of these only two have a modulation index in excess of 0.2. In the MASIV survey of Lovell et al. (2008), of their

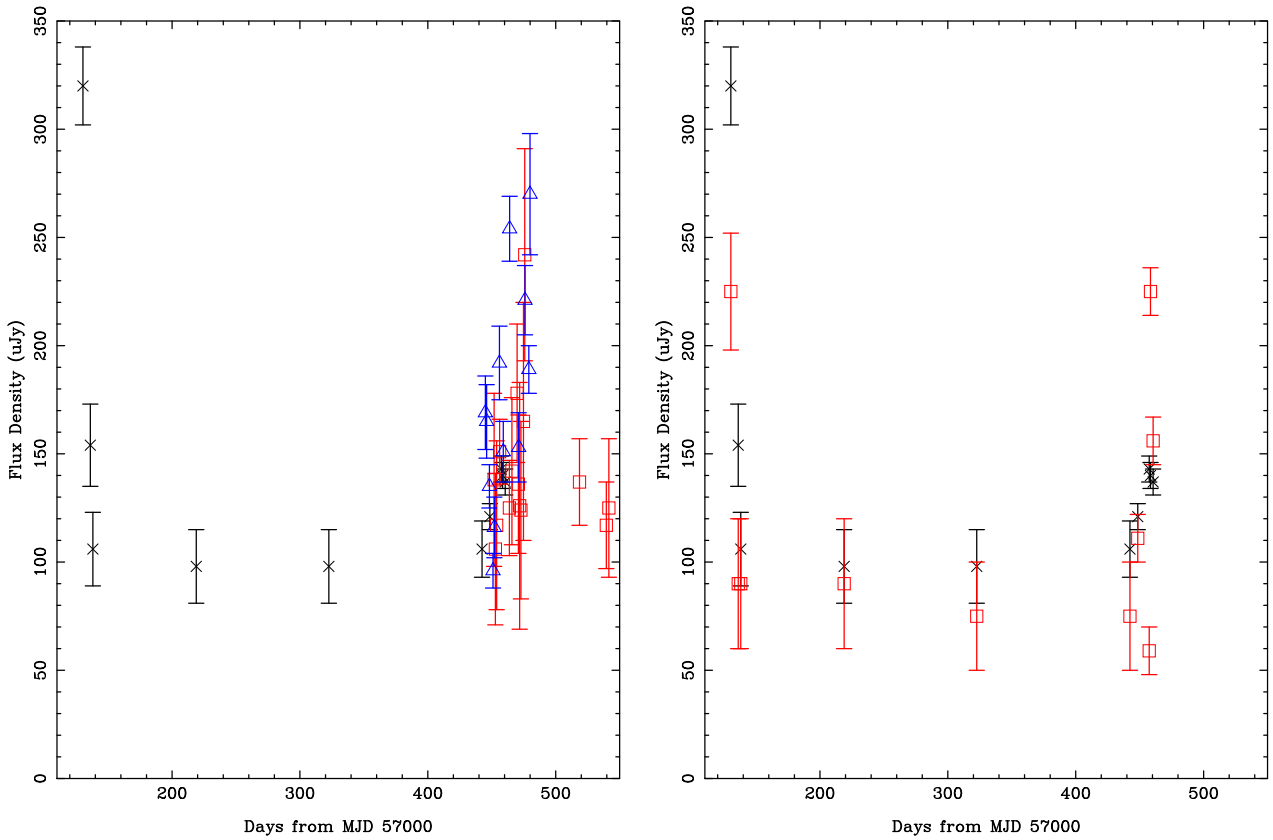

Figure 1. Left-hand panel: radio light curve at 5.5 GHz. Black crosses denote ATCA observations, blue triangles JVLA observations, and red squares VLBA, e-MERLIN and EVN. Right-hand panel: radio light curve from the ATCA data at 5.5(black crosses) and 7.5 GHz (red squares).

443 sources specifically chosen to be a flat spectrum and hence susceptible to variability, only 1 source per epoch showed a modulation index in excess of 0.2. The survey of Mooley et al. (2016) found that 38 out of 3652 sources (∼1 per cent) had modulation indices in excess of 0.26 over the period of a week. The usual caveats apply here; all these surveys were either at a different observing frequency or at a higher flux density limit or both, compared to our data.

4.2 Interstellar scintillation

Bassa et al. (2016) and Giroletti et al. (2016) show that the ATCA radio source (at least at later epochs) is highly compact and located at the centre of the optical galaxy. This indicates that the source is likely an AGN. Although the ∼mas resolution is not sufficient to determine whether the source should undergo interstellar scintillation (ISS), it is certainly indicative. In addition, the quasi-simultaneous observations made by Vedantham et al. (2016) between 1 and 20 GHz indicate that the source has a flat spectral index (modulated by ISS; see Akiyama & Johnson 2016).

We deduce from the observations that the variations may be dominated by refractive scintillation. Diffractive scintillation appears unlikely to be contributing to the flux density variations: At the position of the source, the expected time-scale for diffractive scintillation is $\simeq$10 min, for an assumed scintillation velocity of 50 km s^{-1}, which is much shorter than the time-scale of the fastest variations evident in the light curve. Moreover, we note that diffractive scintillation is only relevant if the source contains structure on scales below ∼0.1μas for the expected scattering properties along this line of sight.

We therefore investigated the probability that the data are consistent with the form of an intensity probability distribution function expected from ISS in the regime of refractive scintillation. This is a Rician distribution (Cohen et al. 1967) with two free parameters, the amplitude of the non-varying component and the amplitude of the scintillation fluctuations. The probability that the 5.5 GHz light curve is drawn from such a distribution is 90 per cent.

Using simple arguments, we would also expect that the modulation index of weak radio sources be higher than those of brighter sources if all AGNs have a brightness temperature near the inverse Compton limit. If this is correct, then the high modulation index we measure for WISE J071634.59−190039.2 compared to sources in, for example, the MASIV survey (Lovell et al. 2008) is to be expected. In addition, the low galactic latitude of WISE J071634.59−190039.2 also likely contributes to the higher modulation index.

We therefore conclude that the variability we see in WISE J071634.59−190039.2 is largely due to ISS with a couple of minor caveats. First, the probability distribution argument does not take into account the time sequence of the data. Although we have no a priori knowledge of what form an afterglow to an FRB might take, the light curve from Keane et al. (2016) is suggestive of a fading radio transient. Indeed, even with the additional data, the probability of getting a value as high as that of the first epoch is only 0.3 per cent. Secondly, ISS in compact AGNs is highly intermittent (Lovell et al. 2008), and the light curve is only sparsely sampled during the first few months.

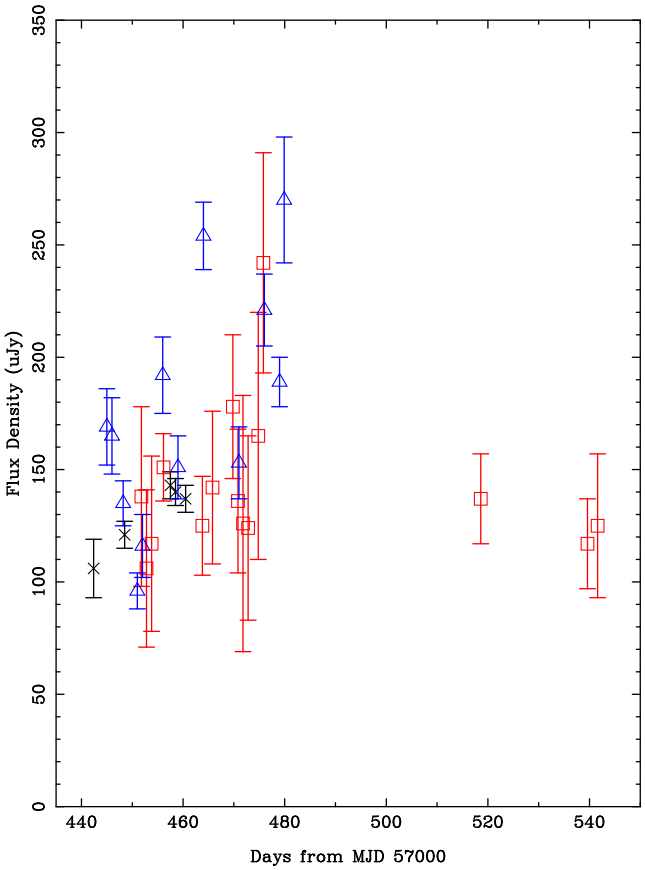

Figure 2. End portion of the radio light curve at 5.5 GHz. Black crosses denote ATCA, blue triangles JVLA and red squares VLBA, EVN or e-MERLIN.

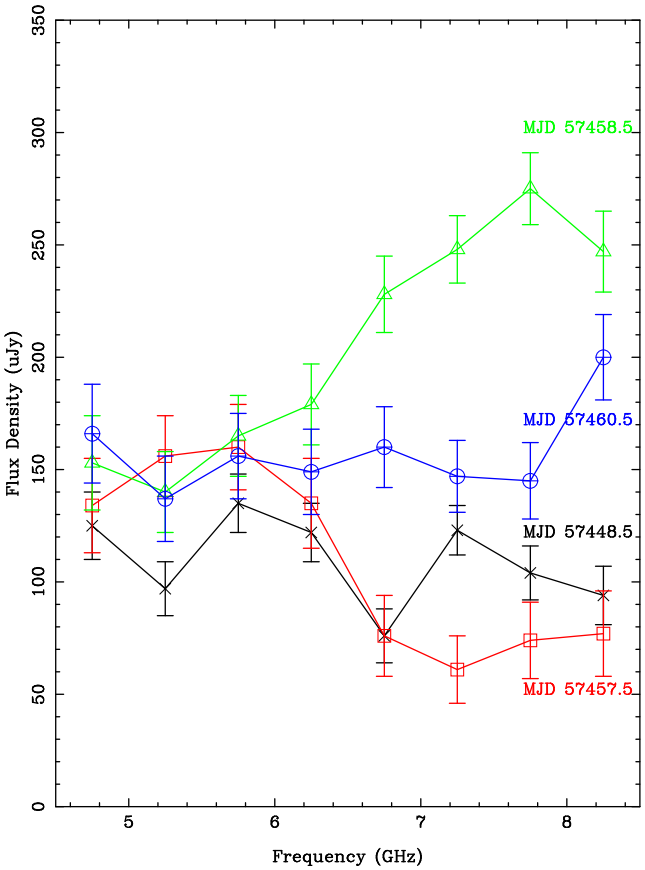

Figure 3. Flux density as a function of frequency for MJDs 574 48.5 (crosses and black line), 574 57.5 (squares and red line), 574 58.5 (triangles and green line) and 574 60.5 (circles and blue line) of the ATCA data.

4.3 Probability arguments

The data obtained by Keane et al. (2016) appeared to show that the radio source was a *transient* (as opposed to a variable). As outlined in Keane et al. (2016), comparison with the Ofek et al. (2011), Mooley et al. (2016) and Bell et al. (2015) surveys yields probabilities of finding such a transient source at significantly less than 1 per cent. Li & Zhang (2016) also provided a compelling chain of logic to show that the probability of seeing the variability of WISE J071634.59−190039.2 is only 0.1 per cent when using the Ofek et al. (2011) survey as a comparison. With the additional data we have obtained for WISE J071634.59−190039.2, it is clear that the source is more correctly described as a *variable*, and the values computed above need to be revisited. In particular, the Mooley et al. (2016) survey showed that some 1 per cent of their sources have a modulation index in excess of 0.26 on time-scales of less than a week.

What then is the probability of detecting a source undergoing ISS in the field of view of the ATCA? The ATCA image covers an area of 0.0625 deg^2 and is roughly complete above 100 μJy; the source counts at this observing frequency above this flux density level are ∼300 deg^{-2} (Huynh et al. 2012). At these flux density levels, star-forming galaxies start to dominate the number counts, and these galaxies do not have strong compact components and will not be seen as ISS variables at our sensitivity. Huynh et al. (2012) estimate that 30 per cent of their sources have flat spectral indices consistent with AGNs, rather than star formation. Finally, not all compact sources that could potentially undergo ISS are actually doing so at any one epoch. Lovell et al. (2008) estimate the incidence of ISS at ∼20 per cent, but the modulation indices of their sources are only of the order of 0.1. Variability with a higher modulation index is rarer although as noted above weaker sources likely modulate more and WISE J071634.59−190039.2 is closer to the Galactic plane than the sources in MASIV. We therefore estimate the incidence of ISS yielding a modulation index in excess of 0.3 to be ∼5 per cent at these Galactic latitudes. We are therefore left with an estimate of 1.5 per cent of all sources, or ∼4.5 sources deg^{-2} above 100 μJy, undergoing ISS at any one epoch. This estimate is not dissimilar to the value given above, obtained by the consideration of the Mooley et al. (2016) survey.

In summary, we estimate that of the order of 1 per cent of all sources at 5.5 GHz at a flux density limit of 100 μJy show variability with a high modulation index on short time-scales. Within the positional error box of FRB 150418, we observe eight sources brighter than 100 μJy, and the probability of observing such a variable source is then ∼8 per cent.

4.4 The variable sky

We have established that the fraction of variable sources, with parameters at 5.5 GHz such as those for WISE J071634.59–190039.2, is ∼1 per cent, both from considering our knowledge of ISS statistics and from the observed number counts of large-scale surveys. Given 300 sourcesdeg^{-2} above 100 μJy at 5.5 GHz, more than 10^5 sources across the entire sky will show variability over the course

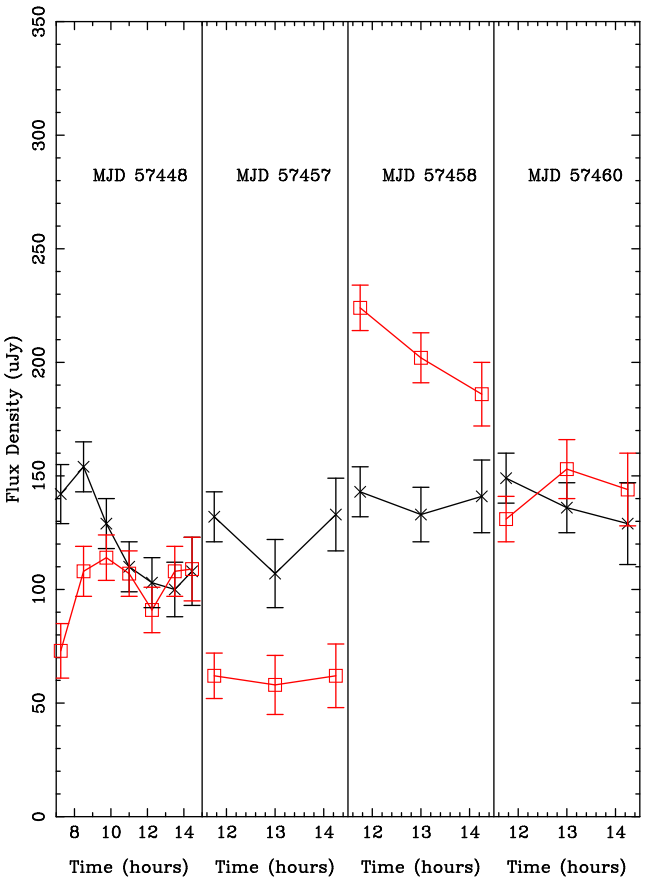

Figure 4. Flux density as a function of time for epochs 7–10. Each panel shows a different epoch with the UT time in hours from the MJD listed at the top of the panel. Points with crosses and black lines denote 5.5 GHz, and points with squares and red lines denote 7.5 GHz.

of one week. This result holds irrespective of the association or not with the FRB.

However, let us for a moment assume an afterglow interpretation for the light curve over the first week. Then, with ∼5000 FRBs per sky per day, any given week would then produce 3.5×10^4 FRB afterglows. We therefore see no obvious disconnect between the number of FRB afterglows and our current knowledge of the variable sky. This is in contrast to Vedantham et al. (2016), who claimed that FRB afterglows must be rare. There are three reasons for this difference. First, Vedantham et al. (2016) assumed a modulation index in excess of 0.7. In light of the data presented here, this value is much too high. They also assumed that the entire flux density from the first epoch was the afterglow, but clearly at least a significant fraction of the emission originates in the underlying AGN. Finally, the volume for FRBs probed with the Parkes telescope is significantly higher than the volume probed for sources similar to WISE J071634.59−190039.2 with the ATCA. If, indeed, we are observing the afterglow to FRB 150418, ATCA follow-up surveys would not detect them if they were significantly more distant than $z \sim 0.5$.

5 CONCLUSIONS

We have combined observations from the ATCA, GMRT, JVLA, e-MERLIN, VLBA and the EVN to show the light curve for the radio source associated with the galaxy WISE J071634.59−190039.2. The source, which Keane et al. (2016) associated with FRB 150418, has, with the acquisition of new data, been shown to be highly variable with a modulation index of 0.36, a time-scale for variability of the order of 1 d and a variable spectral index. These statistics are consistent with those expected from ISS in the weak-scattering regime (Akiyama & Johnson 2016), although the value seen in the first epoch, taken only 2 h after FRB 150418, remains anomalously high. We show that the probability of detecting such a scintillating source in the error box of the FRB is ∼8 per cent, higher than presented in Keane et al. (2016).

Given this information, two possibilities are open. First, the radio source is simply a weak AGN undergoing ISS and is not associated with the FRB. If this is the case, Keane et al. (2016) were unlucky with the low probability of detection, with the high flux density for the first epoch and the time sequence of the light curve. However, this option cannot be ruled out. The second possibility is that the radio source is indeed associated with the FRB. The FRB progenitor would then have to comply with the relatively low level of star formation in the galaxy (Keane et al. 2016). If this is typical for FRBs as a class, we might then expect to see a scintillating AGN in conjunction with an FRB event. Only one other FRB has published follow-up to date (Petroff et al. 2015a), but only a single epoch of ATCA data was obtained. Given the small numbers and our lack of understanding of the progenitors of FRBs, the arguments for or against the association essentially depend on the probability of observing such a strongly variable source within the field of view of the FRB localization. Therefore, the Keane et al. (2016) conclusion is only one of several viable conclusions, the relative probabilities of which are difficult to assess.

With only some 20 FRBs known to date (Petroff et al. 2016), progress in the field requires many more detections and accurate (arcsec) localizations of the bursts themselves, rather than relying on probability arguments as here. By providing the latter, new instruments such as the Canadian Hydrogen Intensity Mapping Experiment (CHIME; Bandura et al. 2014), the Hydrogen Intensity and Real-Time Analysis Experiment (HIREX; Newburgh et al. 2016), the Molonglo Observatory Synthesis Telescope (UTMOST; Bailes et al., in preparation), the Aperture Tile in Focus on Westerbork (APERTIF; Verheijen et al. 2008), MeerTRAP (Stappers & Kramer, in preparation) and TRAPUM on MeerKAT,[1] and the Commensal Real-time ASKAP Fast-Transient Survey (CRAFT; Macquart et al. 2010) on the Australian Square Kilometre Array Pathfinder (ASKAP; DeBoer et al. 2009; Johnston et al. 2008) will undoubtedly break new ground.

ACKNOWLEDGEMENTS

The Parkes telescope and the ATCA are part of the Australia Telescope National Facility, which is funded by the Commonwealth of Australia for operation as a National Facility managed by CSIRO. Parts of this research were conducted by the Australian Research Council Centre of Excellence for All-sky Astrophysics (CAASTRO) through project number CE110001020. Parts of this work were performed on the gSTAR national facility at Swinburne University of Technology. gSTAR is funded by Swinburne and the Australian Government's Education Investment Fund. CGB and EP acknowledge support from the European Research Council under the European Union's Seventh Framework Programme (FP/2007-2013)/ERC Grant Agreement nr. 337062 (DRAGNET; PI Hessels)

[1] http://www.ska.ac.za/science-engineering/meerkat/

and nr. 617199, respectively. We thank Sarah Burke-Spolaor for assistance with the JVLA data reduction, Matthew Bailes for stimulating discussions and the EVN team for providing results prior to publication.

REFERENCES

Akiyama K., Johnson M. D., 2016, ApJ, 824, L3
Bandura K. et al., 2014, Proc. SPIE Conf. Ser. Vol. 9145, Ground-Based and Airborne Telescopes V. SPIE, Bellingham, p. 914522
Bassa C. G. et al., 2016, MNRAS, 463, L36
Bell M. E., Huynh M. T., Hancock P., Murphy T., Gaensler B. M., Burlon D., Trott C., Bannister K., 2015, MNRAS, 450, 4221
Burke-Spolaor S., Bannister K. W., 2014, ApJ, 792, 19
Burke-Spolaor S. et al., 2016, ApJ, 826, 223
Caleb M. et al., 2016, MNRAS, 458, 718
Champion D. J. et al., 2016, MNRAS, 460, L30
Coenen T. et al., 2014, A&A, 570, A60
Cohen M. H., Gundermann E. J., Hardebeck H. E., Sharp L. E., 1967, ApJ, 147, 449
Cordes J. M., Wasserman I., 2016, MNRAS, 457, 232
Cordes J. M., Wharton R. S., Spitler L. G., Chatterjee S., Wasserman I., 2016, preprint (arXiv:e-prints)
DeBoer D. R. et al., 2009, IEEE Proc., 97, 1507
Dennison B., 2014, MNRAS, 443, L11
Falcke H., Rezzolla L., 2014, A&A, 562, A137
Giroletti M., Marcote B., Garrett M. A., Paragi Z., Yang J., Hada K., Muxlow T. W. B., Cheung C. C., 2016, A&A, 593, L16
Hinshaw G. et al., 2013, ApJS, 208, 19
Huynh M. T., Hopkins A. M., Lenc E., Mao M. Y., Middelberg E., Norris R. P., Randall K. E., 2012, MNRAS, 426, 2342
Johnston S. et al., 2008, Exp. Astron., 22, 151
Karastergiou A. et al., 2015, MNRAS, 452, 1254
Katz J. I., 2016, ApJ, 818, 19
Keane E. F., Kramer M., Lyne A. G., Stappers B. W., McLaughlin M. A., 2011, MNRAS, 415, 3065
Keane E. F. et al., 2016, Nature, 530, 453
Law C. J. et al., 2015, ApJ, 807, 16
Li Y., Zhang B., 2016, preprint (arXiv:e-prints)
Loeb A., Shvartzvald Y., Maoz D., 2014, MNRAS, 439, L46
Lorimer D. R., Bailes M., McLaughlin M. A., Narkevic D. J., Crawford F., 2007, Science, 318, 777
Lovell J. E. J. et al., 2008, ApJ, 689, 108
Lyubarsky Y., 2014, MNRAS, 442, L9
Macquart J. P. et al., 2015, Advancing Astrophysics with the Square Kilometre Array (AASKA14), 55
Macquart J.-P., Johnston S., 2015, MNRAS, 451, 3278
Macquart J.-P. et al., 2010, PASA, 27, 272
Masui K. et al., 2015, Nature, 528, 523
McQuinn M., 2014, ApJ, 780, L33
Mooley K. P. et al., 2016, ApJ, 818, 105
Newburgh L. B. et al., 2016, preprint (arXiv:e-prints)
Ofek E. O., Frail D. A., Breslauer B., Kulkarni S. R., Chandra P., Gal-Yam A., Kasliwal M. M., Gehrels N., 2011, ApJ, 740, 65
Petroff E. et al., 2015a, MNRAS, 447, 246
Petroff E. et al., 2015b, MNRAS, 454, 457
Petroff E. et al., 2016, PASA, 33, e045
Rau U., Bhatnagar S., Owen F. N., 2016, AJ, 152, 124
Ravi V., Shannon R. M., Jameson A., 2015, ApJ, 799, L5
Rowlinson A. et al., 2016, MNRAS, 458, 3506
Sault R. J., Teuben P. J., Wright M. C. H., 1995, in Shaw R. A., Payne H. E., Hayes J. J. E., eds, ASP Conf. Ser. Vol. 77, Astronomical Data Analysis Software and Systems IV. Astron. Soc. Pac., San Francisco, p. 433
Scholz P. et al., 2016, preprint (arXiv:e-prints)
Siemion A. P. V. et al., 2012, ApJ, 744, 109
Spitler L. G. et al., 2014, ApJ, 790, 101
Spitler L. G. et al., 2016, Nature, 531, 202
Thornton D. et al., 2013, Science, 341, 53
Tingay S. J. et al., 2015, AJ, 150, 199
Vedantham H. K., Ravi V., Mooley K., Frail D., Hallinan G., Kulkarni S. R., 2016, ApJ, 824, L9
Verheijen M. A. W., Oosterloo T. A., van Cappellen W. A., Bakker L., Ivashina M. V., van der Hulst J. M., 2008, in Minchin R., Momjian E., eds, AIP Conf. Ser. Vol. 1035, The Evolution of Galaxies Through the Neutral Hydrogen Window. Am. Inst. Phys., New York, p. 265
Wayth R. B., Brisken W. F., Deller A. T., Majid W. A., Thompson D. R., Tingay S. J., Wagstaff K. L., 2011, ApJ, 735, 97
Williams P. K. G., Berger E., 2016, ApJ, 821, L22

This paper has been typeset from a TEX/LATEX file prepared by the author.